Base Station Antenna | Directivity | Gain

Technology Reports

Method for Measuring Base Station Antenna Radiation Characteristics in Anechoic Chamber

Base station antennas tend to be long compared to the wavelengths at which they operate. To determine the radiation characteristics of such antennas, measurements must be made in a sufficiently broad space. However, anechoic chambers are typically not large enough to enable measurements to be made from sufficient distances. We have therefore developed a method for precisely determining the radiation characteristics of a base station antenna based on measurements made at insufficient distance from the antenna. This has made it possible to measure the radiation characteristics of base station antennas with ordinary radiation pattern measurement facilities in an anechoic chamber where the results are unaffected by weather.

Research Laboratories

Kazuhiro Komiya

Ryo Yamaguchi

Keizo Cho

1. Introduction

The radiation characteristics (directivity[*1] and gain[*2]) of a mobile terminal base station antenna are important link budget parameters, and it is essential to accurately ascertain whether or not a mobile terminal base station achieves its specified performance. There are many different kinds of base station antennas that are suitable for various frequencies and installation locations, but in general a base station antenna installed outdoors as shown in **Photo 1** has a special shape whereby it is longer in the vertical direction and shorter in the horizontal direction so as to form the desired service area. For example, at the 2 GHz frequency used in IMT (15 cm wavelength), the vertical dimension of a base station antenna will often exceed 2 m.

A long measurement distance is needed to measure the far field[*3] directivity of an antenna that is longer than the wavelength. A generally accepted indicator of the far field distance is $2D^2/\lambda$ (where D is the antenna length and λ is the wavelength), which comes out as approximately 60 m for the measurement distance of the abovementioned base station antenna with a length of 2 m operating at a frequency of 2 GHz. This distance is impossible to achieve in an anechoic chamber[*4] of ordinary size, making it impossible to accurately measure the directivity if measurements are made at distances that fall short of this requirement.

Although this issue can be avoided by making measurements outdoors at a suitable distance, other issues will arise such as the difficulty of obtaining a suitable location and dealing with the effects of weather on the measurement

*1 **Directivity**: One of the radiation characteristics of an antenna. The direction characteristic of the radiation strength from the antenna (or the receiver sensitivity).

results. There are also methods for measuring the directivity inside an anechoic chamber [1][2], but these require additional large-scale special equipment. It is thus not easy to measure the far field directivity of a base station antenna. Furthermore, the manufacturers of base station antennas do not use a uniform method or environment to measure the radiation characteristics of these antennas, so there are likely to be differences in the accuracy of measurements from different manufacturers. It has therefore been necessary to estimate the tolerances that apply to the acceptable specification ranges for base station antennas. Since current base station antennas share frequencies and polarizations*5, and have a complex structure incorporating filters and phase shifters, we need an environment where the radiation characteristics of base station antennas can be verified so that NTT DOCOMO can evaluate and ascertain the performance of these antennas. The authors have therefore developed a method for accurately measuring the radiation characteristics of base station antennas based on measurements made at insufficient distances in an anechoic chamber, which is a facility owned by NTT DOCOMO and the antenna manufacturers. This method considers the special nature of the antenna shape, and involves making measurements at insufficient distances by using a radiation pattern measurement system with a network analyzer and a turntable or the like in an ordinary anechoic chamber to enable far field radiation pattern measurements by computerized synthesis of plane waves based on the acquired data.

Photo 1 Example of an outdoor base station antenna

By introducing this technique, we gained the following benefits:

- Since measurements can be made inside an anechoic chamber, the results are unaffected by weather.
- The synthesis of plane waves at insufficient measurement distances can be implemented by numerical processing using a PC without the need for special equipment, which means this technique can easily be deployed at other measurement locations.

In this way, we were able to realize a standardized measurement method for use by NTT DOCOMO and the antenna manufacturers.

In this article, we describe our basic study of the method for measuring directivity and gain of base station antennas in an anechoic chamber.

2. Measurements Using Synthetic Aperture Array Antenna

2.1 Measurement of Far-field Directivity

Figure 1 shows the principle of measurements using a synthetic aperture array antenna in this method. These

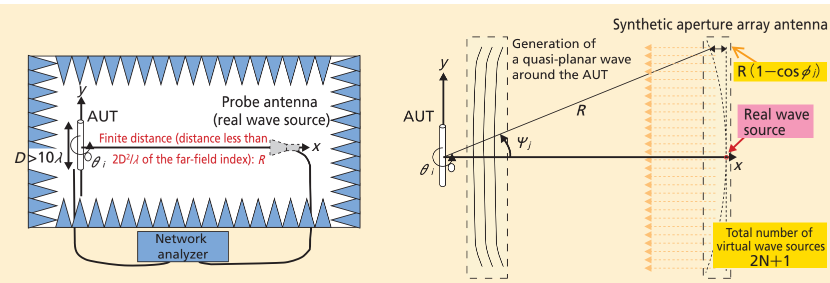

(a) Actual measurement (measurement of electric field pattern at a finite distance in an anechoic chamber)
(b) Virtual measurement (generation of plane waves by numerical processing)

Figure 1 Measurements using a synthetic aperture array antenna

*2 **Gain**: One of the radiation characteristics of an antenna. An indicator of how many times larger the radiation strength in the antenna's direction of peak radiation is relative to a standard antenna.

*3 **Far field**: The region where the electromagnetic field radiated from an antenna is determined only by its direction function and does not depend on the distance to the point of observation.

*4 **Anechoic chamber**: A test facility that is shielded from external radio waves and where the walls, floor and ceiling are covered with an electromagnetic absorbing material to suppress reflections.

measurements are divided into two stages: (a) actual measurements, and (b) virtual measurements.

- Actual measurements: First, as shown in fig. 1(a), the x axis is taken to be the direction facing the broad side[*6] of the Antenna Under Test (AUT) in the anechoic chamber, and the origin O is set corresponding to the center of the antenna. Next, a probe antenna is placed at a measurement distance (hereinafter referred to as "finite distance") R that does not satisfy the far field criteria along the x axis. The AUT is then rotated through an angle θ_i while the complex received electric field[*7] $E_{near}(\theta_i)$ from the probe antenna is measured by a network analyzer and the resulting data is captured by a PC. This process is the same as for ordinary radiation pattern measurements in an anechoic chamber, but the data obtained here is not accurate because the measurement distance is insufficient.
- Virtual measurements (array synthesis): Next, the abovementioned measurements are used in numerical calculations (offline signal processing) to form a virtual synthetic aperture array antenna[*8]. As shown in fig. 1(b), N equally-spaced virtual wave sources are arranged symmetrically on both sides of the probe antenna (the real wave source) to give a total of $2N+1$ virtual wave sources. A characteristic of this technique is that the array antenna is rotated through an angular step of $\Delta\psi$ to form an arc. Since the synthetic aperture array antenna has an arc shape, it is possible to generate a quasi-planar wave[*9] around the AUT (*y*-axis direction) at a finite distance by giving each wave source a phase difference corresponding to the path difference $R(1-\cos\psi_j)$. The far field directivity $E_{far}(\theta_i)$ obtained by taking this phase difference into consideration is obtained by summing the received electric field strengths $E_{near}(\theta_i)$ from each wave source point at the finite distance; i.e., it is obtained by Equation (1) as the synthetic received electric field of the incoming waves from the synthetic aperture array antenna.

$$E_{far}(\theta_i)=\sum_{j=-N}^{N}E_{near}(\theta_i+\psi_j)w_i \exp\{jkR(1-\cos\psi_j)\}\Delta\psi \qquad (1)$$

Here, $E_{far}(\theta_i)$ is the complex far field that we want to determine, $E_{near}(\theta_i+\psi_j)$ is the complex received electric field from each wave source at the finite distance (transmission characteristics), w_j is the array synthesis weighting, R is the measurement distance, ψ_j is the relative angle of the *j*th wave source position, $\Delta\psi$ is the angular step of the placement of virtual wave sources, and $k\ (=2\pi/\lambda)$ is the wave number. If the angular points obtained from the rotation angles θ_i and relative angles ψ_j (the sample points during the measurement) are set at the same positions, then there is no need to re-measure $E_{near}(\theta_i+\psi_j)$ once $E_{near}(\theta_i)$ has been measured. In other words, $E_{near}(\theta_i)$ only needs to be measured once in the circumferential direction. In Equation (1), the phase term $R(1-\cos\psi_j)$ is not the phase of excitation[*10] during the actual measurements, but a virtual term used in array synthesis to express the phase correction of differential routes from each constituent element (wave source) of the synthetic aperture array antenna as described above.

2.2 Gain Measurement

In the proposed technique, gain measurements are performed by a method where a REFerence antenna (REF) of known gain is substituted for and compared with the AUT at the same point (called a gain transfer method). Since the REF and AUT must be substituted into the same measurement environment, the REF must acquire the complex received electric field $E_{near}(\theta_i)$ by the same procedure as the AUT—i.e., by performing rotational measurements—regardless of its aperture size.

In the gain transfer method, if the probe antenna is on the transmitting side and the REF and AUT are on the

*5 **Polarization**: The direction in which electric waves oscillate as they propagate through space. The base station antennas considered in this article are often configured to use both horizontal and vertical polarization.

*6 **Broad side**: In an antenna where there are multiple elements arranged along a straight line, this is the direction at right angles to the axis of the arrangement.

*7 **Complex received electric field**: The received electric field expressed in complex notation. An electric field can be expressed by a complex number consisting of the amplitude and phase.

*8 **Array antenna**: An antenna consisting of a matrix of multiple elements.

receiving side, then the gain G^{AUT} in the desired direction is obtained from the following equation:

$$G^{AUT} = G^{REF} P^{AUT} / P^{REF} = G^{REF} (E_{far}^{AUT} / E_{far}^{REF})^2 \quad (2)$$

Here, G^{REF}, P^{AUT}, P^{REF}, E_{far}^{AUT} and E_{far}^{REF} are, respectively, the known gain of REF, the received power of AUT, the received power of REF, the received electric field strength of AUT obtained from Equation (1), and the received electric field strength of REF obtained from Equation (1).

3. Verifying the Effectiveness of Far Field Radiation Pattern Measurements

3.1 Validation by Method of Moments

To verify the effectiveness of this method, we performed a simulation by the method of moments[*11] corresponding to a test at a finite distance. As an example of AUT we used a half-wave dipole array antenna with excitation of equal amplitude, and we calculated the electric field distribution at a measurement distance of 10 m with the computer simulation specifications shown in **Table 1**. Here, for convenience, the AUT was treated as the transmitting antenna, and the probe antenna itself was not modeled but instead the complex value of the electric field at the measurement point was used directly (which corresponds to regarding the probe antenna as non-directional). At the same time, we also calculated the far field directivity. As a representation of the relative directivity where the results are normalized by the maximum values, **Figure 2**(a) shows the finite distance electric field directivity together with the far field directivity. In particular, there is a pronounced discrepancy in the vicinity of the main beam[*12], which confirms that it is not possible to accurately measure the far field directivity with finite distance measurements.

Next, fig. 2(b) shows the results obtained by array synthesis of finite distance electric fields by this method, together with the far field directivity. Here, the weightings of the wave sources in Equation (1) are all taken to be 1, and only phase correction was performed. From the figure, there was a slight discrepancy between the values in the end-fire[*13] direction, but the main beam shapes were in close agreement.

From the above, by using this technique we were able to confirm that the far-field radiation pattern can be obtained to a high degree of accuracy based on finite distance measurements.

3.2 Evaluation of Plane Wave Accuracy and Measurement Distance

Since this technique requires that virtual quasi-planar waves are generated around the AUT, it is thought that the precision with which these waves are generated will have a direct effect on the measurement parameter settings.

Table 1 Computer simulation specifications

Frequency	2.0 GHz
AUT	Half-wave dipole array antenna
Length of AUT	2.1 m
Measurement distance	10 m
Opening angle of synthetic aperture	150°
Number of elements in synthetic aperture	375
Step angle of the synthetic aperture	0.4°

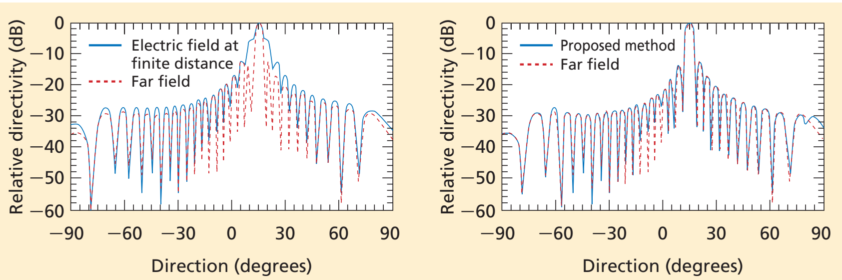

Figure 2 Results of radiation pattern verification by simulation

*9 **Plane wave**: An electromagnetic wave where the amplitude and phase of the electromagnetic field are constant within a plane perpendicular to the propagation direction.

*10 **Excitation**: Supplying electricity to an antenna to generate electromagnetic waves.

*11 **Method of moments**: An electromagnetic field analysis method that can efficiently measure electrical currents flowing in metals, and can thereby be used to calculate the direction in which an electromagnetic wave is radiating.

*12 **Main beam**: The beam in the direction of strongest radiation.

*13 **End-fire**: The axial direction in an antenna whose elements are arranged in a straight line.

Here, to clarify the factors that facilitate far field measurements, we clarified the basic characteristics of this technique by conducting a simulation to quantitatively evaluate the precision (amplitude distribution and phase distribution) with which plane waves are generated around the AUT.

Table 2 shows the specifications of the plane wave evaluation simulation. Here, on the wave source side, a numerical superposition of the amplitude and phase distributions from each wave source is used to obtain the synthetic electric field $E_{AUT}(x, y)$ around the AUT. For simplicity, each wave source is treated as a point wave source.

In an ordinary radiation pattern measurement system, the probe antenna is a single wave source. In this case, **Figure 3** shows the electric field distribution around the AUT for measurement distances of $R=60$ m and 10 m. As the figure shows, the measurement conditions with a single wave source are limited not by the amplitude distribution but by the phase distribution which varies sharply.

Next, we will evaluate the characteristics when this method is applied. **Figure 4** shows the electric field distribution around the AUT when the amount of wave source spreading equivalent to the proposed technique (forming a virtual synthetic aperture array antenna) was 150° with the measurement distance still at $R=10$ m. Compared with the case of the single probe antenna (an ordinary radiation pattern measurement system) in fig. 3, the deviation of the amplitude distribution was larger and oscillated with a period roughly equal to one wavelength with a maximum deviation of approximately 0.6 dB. This oscillation indicates the presence of standing waves, which means the wavefronts were not completely planar due to the insufficient distance from the synthetic aperture array antenna. A similar yet small periodic fluctuation was also seen in the phase distribution, but the absolute value of the deviation was much smaller than that of fig. 3, was suppressed within 5°, and had very little positional dependence. The suppression of this phase deviation is thought to be an effect of using the synthetic aperture array antenna. The figure also shows the values for the case where $R=5$ m.

Table 2 Plane wave evaluation simulation specifications

Frequency	2.0 GHz
AUT	Point wave source
Measurement distance	10 m
Opening angle of synthetic aperture	150°
Number of elements in synthetic aperture	1,501
Step angle of the synthetic aperture	0.1°

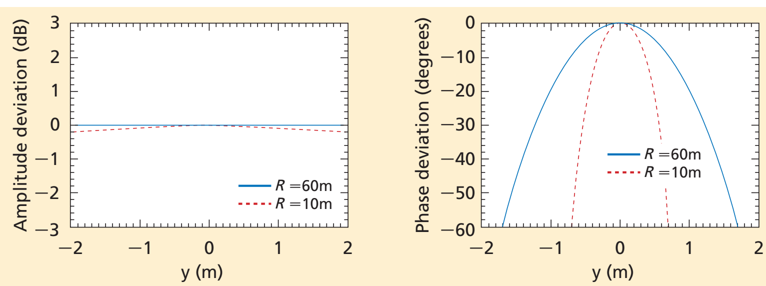

(a) Amplitude (b) Phase

Figure 3 Electric field distribution around the AUT (single wave source at probe)

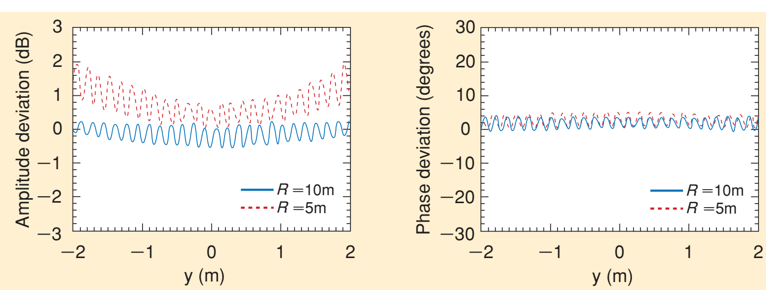

(a) Amplitude (b) Phase

Figure 4 Electric field distribution around the AUT (applying the proposed method)

It can be seen that the shorter measurement distance is acceptable with regard to the phase characteristics which show no large variation, but causes a large degradation of the amplitude distribution.

Figure 5 shows how the amplitude characteristics and phase characteristics of the plane wave electric field distribution vary with the measurement distance. For both parameters, the worst-case values of the difference between the maximum and minimum values are plotted. The amplitude discrepancy increases as the measurement distance becomes smaller, reaching almost 1 dB at a distance of 5 m. On the other hand, the phase characteristics have good characteristics within 10° at almost all measurement distances.

From the above results, it can be said that although using this technique causes alight degradation of the amplitude characteristics, the phase characteristics can be markedly improved, thereby enabling far-field radiation pattern measurements to be made even at finite distances.

4. Verifying the Effectiveness of Gain Measurements

4.1 Evaluation of Measurement Distance by the Method of Moments

As in the far-field radiation pattern measurements, since the distance to the synthetic aperture array antenna is thought to affect the accuracy of gain measurements, we used the method of moments to conduct a verification using the measurement distance between the transmitted and receiver as a parameter. **Table 3** shows the specifications of the gain evaluation simulation. The measurement distance R and the angular step $\Delta\phi$ of the virtual wave source are related by the following formula, where ΔL is the distance between the virtual wave source elements ($R \gg \Delta L$):

$$\Delta\phi = \Delta L/R \qquad (3)$$

This means that when R is large, $\Delta\phi$ must be made small. In this verification, we chose $\Delta\phi = 0.2°$ considering the angular step setting of the ordinary radiation pattern measurement system.

As the results of this verification analysis, **Figure 6** shows how the gain varies with the measurement distance. Here, the horizontal axis shows the measurement distance between the transmitter and receiver (up to 14 m), and the vertical axis shows the amount of gain fluctuation with respect to the directional gain calculated from the power radiated in all directions in the far field of the AUT. It can be seen that when the measurement between the transmitter and receiver is 6 m or more, the deviation can be kept within 0.1 dB. On the other hand, when the measure-

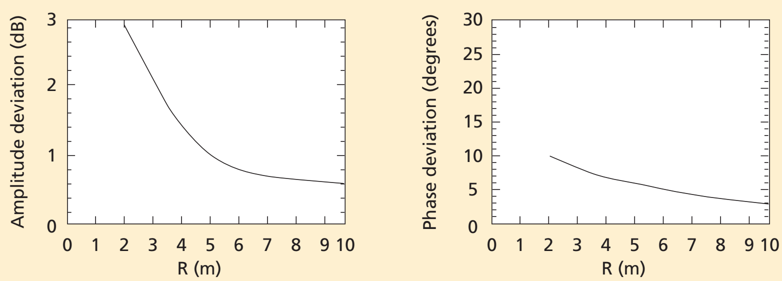

(a) Amplitude (b) Phase

Figure 5 Variation of plane wave field distribution with measurement distance

Table 3 Gain evaluation simulation specifications

Frequency	2.0 GHz
Reference antenna	Half-wave dipole antenna
Antenna under test	Half-wave dipole array antenna
Length of antenna under test	2.1 m
Measurement distance	10 m
Opening angle of synthetic aperture	150°
Number of elements in synthetic aperture	751
Step angle of the synthetic aperture	0.2°

ment between the transmitted and receiver is smaller, the gain fluctuations increase. This is thought to be because the amplitude deviation around the AUT becomes larger as the distance decreases as shown in fig. 4, so a quasi-planar wave can no longer be generated.

4.2 Measured Evaluation of Gain Errors Arising from the Effects of a Reference Antenna

As mentioned above, in gain measurements by the gain transfer method, it is necessary to measure a REF of known gain. Normally, a standard horn antenna[*14] is used as the REF for the frequency bands used in mobile communication, but here we used a REF with directivity similar to that of the AUT, and we used NTT DOCOMO's anechoic chamber (distance between transmitted and receiver: 10 m) to measure the gain fluctuation characteristics with regard to positional accuracy arising during antenna installation.

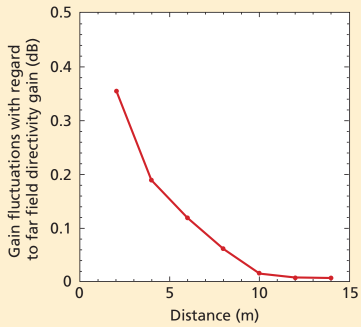

Figure 6 Variation of gain with measurement distance

The measurement specifications are shown in **Table 4**. Measurements were made with the center of REF varied from the origin in the front-to-back (*dx*), left-to-right (*dy*) and height (+*dz*) directions relative to the probe antenna. Due to constraints on the size of the turntable and the stability of the installation, the maximum values of the offset positions were different between the three parameters. In this case, the conversion according to Equation (1) was performed under the assumption that the center of REF was at the origin. **Figure 7** shows the gain fluctuations with regard to positional accuracy. The graph is normalized to the gain value obtained when the center is positioned at the origin. It can be seen that *dx* is the parameter for which the difference in gain fluctuations is the largest. This is thought to be because of fluctuations corresponding to the distance characteristics. On the other hand, parameters *dy* and *dz* have smaller gain fluctuations than *dx*. This is thought to be because an antenna that is long with regard to the wavelength is used for REF as well as for AUT, thus mitigating the effects of reflections occurring in the anechoic chamber due to array synthesis. From the figure, it can be seen that in this anechoic chamber it is possible to perform measurements with a gain variation of approximately 0.2 dB by keeping the installation precision to within an error of 10 cm or less.

Table 4 Measurement specifications of gain fluctuations with regard to positional

Frequency	2.0 GHz
Antenna under test / Reference antenna	Half-wave dipole array antenna
Length of antenna under test / reference antenna	2.1 m
Measurement distance	10 m
Opening angle of synthetic aperture	150°
Number of elements in synthetic aperture	1,501
Step angle of the synthetic aperture	0.1°

5. Conclusion

In this article, we have described our basic study of the radiation characteristics of a base station antenna in an anechoic chamber. Based on electromagnetic simulation and actual measurement tests in an anechoic chamber, we have revealed that this technique can be used to make accurate measurements of the far field radiation pattern

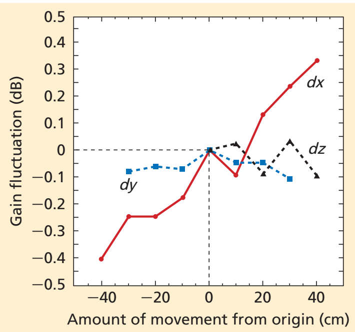

Figure 7 Gain fluctuations with regard to positional accuracy

*14 **Standard horn antenna**: An antenna that provides a standard gain. Normally a horn antenna consisting of a waveguide flared at one end is used.

and gain of an antenna whose length is larger than the wavelength. In this article we performed our investigation with a 2 GHz band vertically polarized antenna, but the same technique can also be used for measurements at other frequency bands or with horizontal polarization. In the future, in order to apply this technique to the measurement sites of antenna manufacturers, we plan to evaluate the measurement precision in the anechoic chambers of various companies, and to reflect the results in optimization of the specification pass ranges of base station antennas.

REFERENCES

[1] R.C. Johnson, H.A. Ecker and R. A. Moore: "Compact range techniques and measurements," IEEE Trans. Antennas and Propagation, Vol. AP-17, No.5, pp.568-576, Sep. 1969.

[2] J. E. Hansen: "Spherical Near-field Antenna Measurements," Peter Peregrinus Ltd., London, 1988.